ARMY RESEARCH LABORATORY

Feasibility Study of a Smart Submunition: Deployment From a Conventional Weapon

Norman M. Wereley
Darryll J. Pines

ARL-CR-0475 JUNE 2001

prepared by

Smart Structures Laboratory
Alfred Gessow Rotorcraft Center
Department of Aerospace Engineering
University of Maryland
College Park, MD 20742

under contract

DAAD19-00-1-0127

Army Research Laboratory
Aberdeen Proving Ground, MD 21005-5066

ARL-CR-0475 June 2001

Feasibility Study of a Smart Submunition: Deployment From a Conventional Weapon

prepared by

Norman M. Wereley
Darryll J. Pines
University of Maryland

under contract

DAAD19-00-1-0127

Abstract

This report details the smart autonomous rotorcraft submunition (SMARS) designed for deployment from a conventional munition. SMARS was developed in response to requirements defined in an initial meeting with Mr. Michael Hollis of the U.S. Army Research Laboratory, Aberdeen Proving Ground, Maryland, April 18, 2000.

The primary goal of this initial design was to develop a rotorcraft that could be housed inside a conventional munition and carry a payload of 1.36 kg for a period of 20 minutes. The vehicle must be capable of scanning an area equivalent to 5 square kilometers. The proposed design in this report satisfies these requirements.

The final design concept consists of a coaxial rotorcraft with a 0.6096-m (2-foot) rotor diameter weighing 6 kg. The rotors are rigid in flight; the swashplate was eliminated to reduce complexity. However, the blades are able to fold at the root in order to meet packaging requirements.

A small-scale prototype called "miniature coaxial rotorcraft" (MICOR) was developed and flight tested to show the feasibility of the concept and validate the yaw and altitude control systems. Scaling laws were developed to ensure that the characteristics of MICOR could be applied to SMARS. In addition, a deployment feasibility study was performed. A simple small-scale rotorcraft was manufactured, which was launched and deployed by a high-powered model rocket to demonstrate the feasibility of the SMARS concept.

Contents

1. **Introduction** 1

2. **Requirements** 1
   - 2.1 Mission Profile 1
   - 2.2 Vehicle Specifications 2

3. **Concept Selection** 3

4. **Feasibility Study** 3
   - 4.1 Hover 3
   - 4.2 Propulsion System Availability 4
   - 4.3 Critical Design Issues 4

5. **Preliminary Design** 5
   - 5.1 Configuration 5
   - 5.2 Low Reynolds Number Airfoil 11
   - 5.3 Coaxial Rotor Design 11
   - 5.4 Propulsion System 12
   - 5.5 Vehicular Parameters 14
   - 5.6 Packaging and Deployment 15
   - 5.7 Flight Control 16

6. **Small-Scale Prototype Study (MICOR)** 19
   - 6.1 Vehicle 19
   - 6.2 Tethered Flight Test 21
   - 6.3 Lateral Control and Scaling 22

7. **Deployment Feasibility Study** 25
   - 7.1 Vehicular Parameters 26
   - 7.2 Launch System 27
   - 7.3 Flight Test 28

8. **Conclusion** 28

References 31

Distribution List 33

Report Documentation Page 35

Figures

1. Typical Mission Profile 2
2. Slalom Mission Profile 2

3. Single Rotor Configurations 7
4. Twin Rotor Configurations 7
5. Quad Rotor Configurations 7
6. Other Flying/Test Bed Rotorcraft Configurations 7
7. Airfoil AGRC 1506 12
8. Lithium-Ion Battery Discharge Characteristics 13
9. SMARS With No Lateral Control 14
10. SMARS in Stowed Configuration 15
11. SMARS' Deployment Scheme 16
12. SMARS' Transmission Configuration 17
13. Aerodynamic Flaps 17
14. Gimballed Drive Train/Rotor 18
15. Ducted Propeller With Reaction Jets 18
16. MICOR 20
17. Blade Mold Parts 20
18. Final SMARS' Transmission Configuration 21
19. Tethered Flight Test 22
20. SMARS Test Vehicle 26
21. SMARS Test Vehicle in Stowed Configuration 26
22. Launch Rocket 27
23. Test Vehicle Stowed in the Rocket Nose Cone 27

Tables

1. Selection Criteria 6
2. Single Rotor Configurations 8
3. Twin Rotor Configurations 8
4. Multi-Rotor Configurations 9
5. Other Helicopter Configurations 9
6. Coaxial Rotor Characteristics 12
7. SMARS' Vehicular Parameters 14

FEASIBILITY STUDY OF A SMART SUBMUNITION:
DEPLOYMENT FROM A CONVENTIONAL WEAPON

1. Introduction

This report details the smart autonomous rotorcraft submunition (SMARS) designed for deployment from a conventional munition. SMARS was developed in response to requirements defined in an initial meeting with Michael Hollis of the Advanced Munitions Concepts Branch, Weapons and Materials Research Directorate, of the U.S. Army Research Laboratory (ARL) on April 18, 2000.

2. Requirements

The requirements used for the design and analyses of the SMARS vehicle are those specified in Amendment 2 of the fiscal year 2000 broad agency announcement (BAA).

2.1 Mission Profile

The "smart" submunition is intended to perform the following mission. The mechanism shall be ejected from the projectile at an altitude of 3.5 km, with a velocity of ~Mach 1. At 2.5 km, the smart submunition shall be fully deployed and functional. At this point, the smart submunition will have the capability for guided flight to a particular location on the ground.

The smart submunition must fly or glide the payload to the ground in a set flight pattern that covers 5 square kilometers (km^2). For example, a spiral pattern with a radius of 1.26 km is acceptable. A slalom-type pattern and a degenerating spiral pattern are other examples. The flight pattern must be interruptible by radio control.

The requirement specified in the BAA is surveillance of a 5-km^2 area following deployment. Figures 1 and 2 show two potential mission profiles. The first profile consists of a circular area 1.26 km in diameter; the second is a slalom pattern that covers a rectangular area 2.5 km by 2 km.

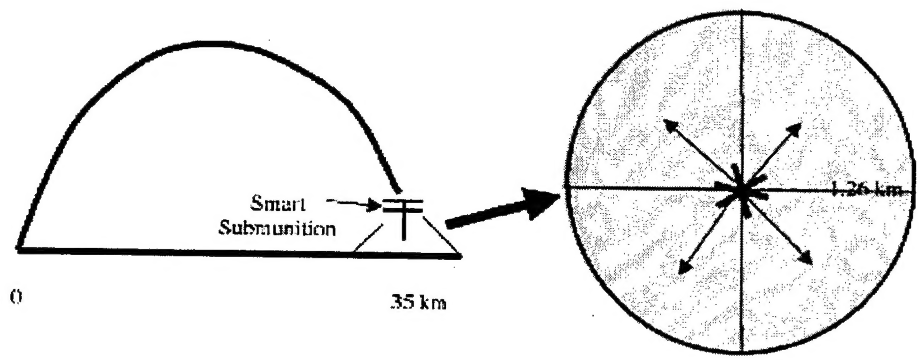

Figure 1. Typical Mission Profile.

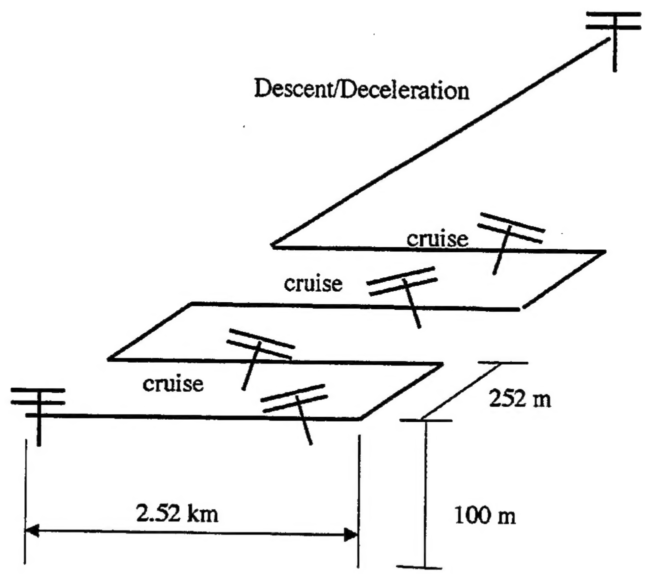

Figure 2. Slalom Mission Profile.

2.2 Vehicular Specifications

The vehicular specifications, including size and performance requirements, are presented in Amendment 2 of the BAA:

1. Volumetric constraints. The smart submunition is placed within an artillery shell. The diameter of the smart submunition shall be no more than 147.8 mm (5.82 in.), and the length of the mechanism shall be no more that 406.4 mm (16 in.).

2. The smart submunition must be projected to sustain artillery gun launch and free flight loads: (a) 16,000 g's of axial inertial load over 15 ms, (b) 10 Hz of initial spin, and (c) 4,800 g's of transverse load attributable to "balloting[1]".

[1]Balloting can be decomposed into two types of motion: a *translation* of the center of gravity (CG) perpendicular to the line of fire, and an *angular* rate about the CG.

3. The smart submunition must sustain loads caused by ejection from the artillery shell, approximately 7,500 g's opposite to the direction of artillery shell motion. The artillery shell shall have a velocity of about Mach 1 before ejection.

4. The smart submunition must incorporate a payload weighing 1.36 kg (3 lb) and a contiguous volume of 695 cm^3 (42.4 in^3).

5. A glide ratio of 1 meter vertical to 10 meters horizontal or better is required, with wind speeds as great as 10 knots.

6. Offeror(s) shall provide an initial packaging design based on the volumetric constraints, as contained in Specification 1 of the BAA.

3. Concept Selection

Given the mission specifications, it was decided that the baseline micro-air vehicle (MAV) design would be restricted to a rotary wing configuration. A rotary wing vehicle would be able to easily fly the mission profile and would allow greater flexibility than a fixed wing vehicle for the operator to investigate a specific item of interest since the restriction of a minimum forward flight speed is not present. Additionally, a rotorcraft would be better able to handle situations when obstacle avoidance is a requirement.

4. Feasibility Study

Before the preliminary design is initiated, the feasibility of meeting basic mission requirements with a rotary wing vehicle must first be addressed. Most importantly, it must be determined whether a propulsion system exists that is able to deliver sufficient power to meet the mission objectives. For this research, an assessment must also be made about whether a vehicle can be designed to withstand the large loads specified in the BAA. Once these issues are addressed, the preliminary design phase can begin.

4.1 Hover

The hover power analysis was performed for the case of a single main rotor. The results are then easily extended to other rotor configurations. Assumptions were made for the basic vehicular parameters, based on the specifications provided in the BAA. These assumptions are

- Tip Mach number = 0.2
- Blade solidity = 0.16
- Vehicle gross take-off mass = 5 to 10 kg
- C_{d0} = 0.04 (low Reynolds number airfoil, 80,000)
- Maximum rotor radius = 0.4064 m
- Flight duration = 30 minutes

The maximum rotor radius was chosen to be equal to the length of the vehicle specified in the BAA. This would be the maximum length of a single blade in its stowed configuration, assuming a single hinge point at the root of the blade. A relatively high C_{d0} value was chosen because of the highly viscous nature of low Reynolds number airfoils.

The following methodology was used to determine the power requirements of the vehicle just specified:

- Momentum theory calculations were performed in hover.
- Detailed blade element theory calculations were performed in hover.
- Low Reynolds number effects were incorporated into the estimates.

Calculations were performed for different values of rotor radius and gross weight. Results indicated that a vehicle with a rotor radius of 0.4064 m (16 in.) could hover with a gross take-off weight of approximately 5.3 kg. The minimum power required to hover was determined to be approximately 403 w. Thus, given the required flight duration, a required total mission energy of 200 watt-hours (wh) was calculated.

4.2 Propulsion System Availability

Lithium-ion batteries have specific energy values of 150 to 250 wh/kg. Thus, with 150-wh/kg batteries, batteries weighing a total of 1.34 kg are required to maintain hover and/or cruise flight conditions for the mission.

4.3 Critical Design Issues

The primary challenges associated with deploying a rotorcraft from a munition stem from the large loads applied to the vehicle during launch and deployment. These loads, as specified by the BAA, include

- Survivability under 16,000-g loading for a period of 15 ms
- Spin rates as great as 10 Hz
- 4800 g's of transverse load attributable to balloting
- Ejection loads of 7,500 g's
- Stabilized flight after deployment at an altitude of 3.5 km and a velocity of Mach 1

Ensuring vehicle survival during these conditions is challenging. However, it is felt that from a structural and electronics perspective, the vehicle can be designed to meet these requirements.

Additional design challenges include

- Design of efficient and effective low Reynolds airfoils for good hover performance;
- Storage scheme for stowing rotorcraft blades;
- Structure and material selection to reduce weight of system and increase payload mass fraction.

The authors believe that these design challenges can be met.

5. Preliminary Design

The preliminary design of the SMARS vehicle is focused on the following areas:

- Configuration selection,
- Low Reynolds number airfoil development,
- Propulsion system,
- Flight control system, and
- Packaging and deployment.

Each of these areas is considered in the following sections.

5.1 Configuration

Selection of a configuration for the SMARS vehicle is based on the systematic selection strategy used in the University of Maryland helicopter design class [1]. A comparative study of the performance of different configurations for the given mission criteria was performed.

5.1.1 Selection Criteria

The design of rotorcraft to be launched as payload in a 155-mm submunition imposes unconventional constraints on the configuration because of the small internal volume, the launch loads, and the intricacies of the mission plan. "Brainstorming" sessions generated a number of candidate configurations and the criteria for evaluating their suitability. Table 1 shows the selection criteria and their respective weights.

The volume inside the 155-mm shell that houses the rotorcraft for its launch mission phase is restricted. Thus, the ability to fold the rotorcraft is a primary design criterion. Reliability is an important consideration to ensure a sufficient rate of mission success, particularly given the severe loading environment

encountered by the vehicle during launch and deployment. Aerodynamic cleanliness, hover efficiency, and cruise efficiency are included to ensure that the aircraft is at its best for all the different flight scenarios in the mission profile. Since this would be the first rotorcraft to be carried in a 155-mm shell, a technologically mature rotorcraft configuration would be preferred to an experimental configuration in order to minimize risk.

Table 1. Selection Criteria

Selection Criteria	Weight
Compactness of folding	10
Reliability	10
Controllability	8
Aerodynamic cleanliness	6
Maturity of technology	10
Hover efficiency	8
Aerodynamic interaction	3
Vibration	8
Cruise efficiency	7
Maneuverability	3
Ease of payload packaging	9
Simplicity of structure	10
Simplicity of control system	8

A payload of electronic instruments must be carried for a successful mission. Some configurations have greater restrictions on size and shape of the payload. Thus, this criterion is also considered in the final selection. Since the rotorcraft is to be remotely piloted, the inclusion of controllability and maneuverability as selection criteria is necessary. Simplicity of the overall structure and control system must also be considered for final selection.

5.1.2 Configuration Evaluation

Schematics of 15 different candidate rotorcraft configurations are given in Figures 3, 4, 5, and 6. The configurations being considered are segregated into four categories: single rotor configurations, twin rotor configurations, quad rotor configurations, and flying/test bed hybrid rotorcraft configurations. Tables 2, 3, 4, and 5 show comparative rankings of the different configurations, based on the selection criteria and their weight.

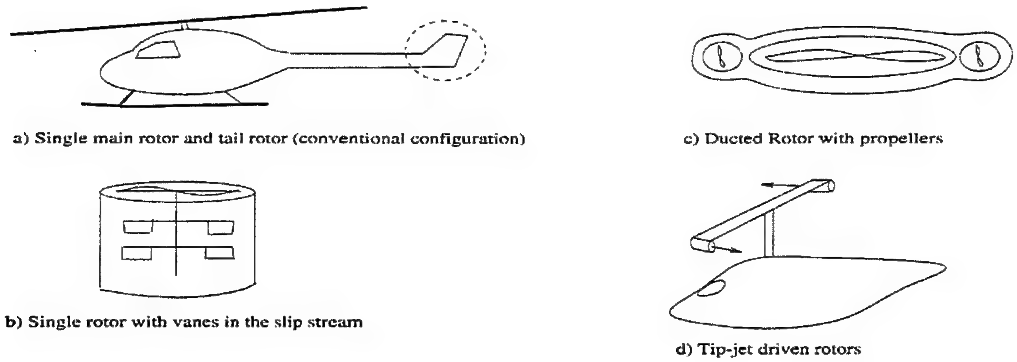

Figure 3. Single Rotor Configurations.

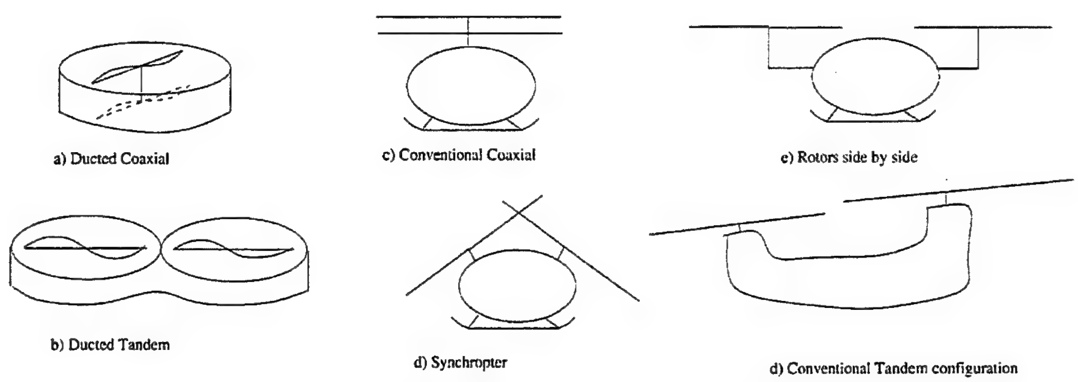

Figure 4. Twin Rotor Configurations.

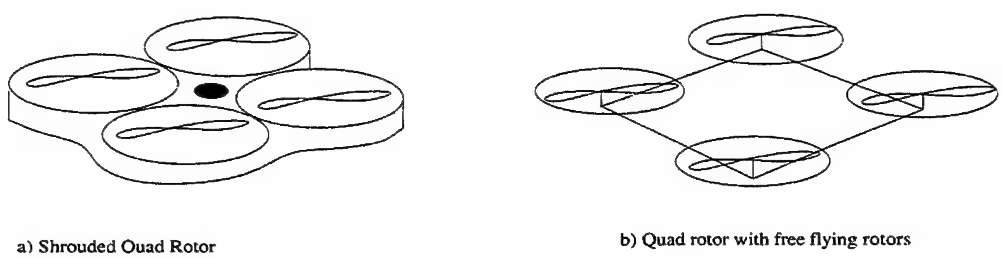

Figure 5. Quad Rotor Configurations.

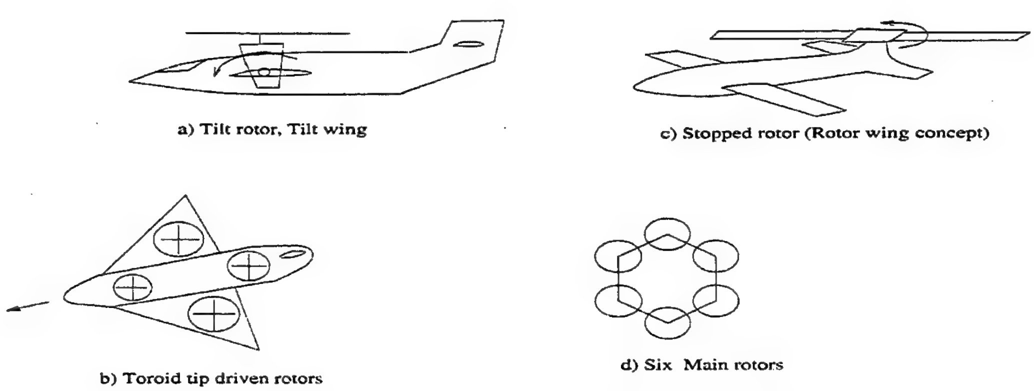

Figure 6. Flying/Test Bed Hybrid Rotorcraft Configurations.

Table 2. Single Rotor Configurations

Weight	Selection Criteria	Conventional	Ducted With Two Propellers	Ducted With Slipstream[a] Vanes	Tip-jet Rotors
10	Compactness of folding	1	2	2	1
10	Reliability	9	5	3	5
8	Controllability	5	3	1	1
6	Aerodynamic cleanliness	8	2	2	3
8	Maturity of technology	10	2	5	2
8	Hover efficiency	10	7	3	8
3	Aerodynamic interaction	7	10	10	9
8	Vibration	1	2	6	3
7	Cruise efficiency	7	4	1	4
3	Maneuverability	5	1	1	3
9	Ease of payload packaging	10	5	1	10
10	Simplicity of structure	8	2	5	10
8	Simplicity of control system	6	2	2	6
	Total	659	336	297	492

[a]Slipstream: a stream of air driven aft by a propeller

Table 3. Twin Rotor Configurations

Weight	Selection Criteria	Side by Side	Tandem	Coaxial	Ducted Coaxial
10	Compactness of folding	2	2	10	2
10	Reliability	8	8	8	10
8	Controllability	5	5	7	5
6	Aerodynamic cleanliness	6	6	8	2
8	Maturity of technology	9	10	10	8
8	Hover efficiency	10	10	8	8
3	Aerodynamic interaction	10	10	7	7
8	Vibration	2	2	1	2
7	Cruise efficiency	6	6	8	6
3	Maneuverability	4	4	3	3
9	Ease of payload packaging	10	10	10	8
10	Simplicity of structure	8	8	10	8
8	Simplicity of control system	6	6	6	6
	Total	646	654	760	588

5.1.2.1 Single Rotor Configurations

The single rotor configurations studied are conventional main rotor-tail rotor configurations, ducted rotors with vanes in the slipstream for providing anti-torque [2], ducted main rotor with propellers for anti-torque and forward speed

[3], and tip-jet driven rotors [4]. The first three of these configurations have been successfully tested for unmanned aerial vehicles (UAVs) [2,5,6,7].

Table 4. Multi-Rotor Configurations

Weight	Selection Criteria	Quad-rotor (shrouded)	Quad-rotor (free)	Six Rotors
10	Compactness of folding	8	8	1
10	Reliability	9	9	1
8	Controllability	8	10	8
6	Aerodynamic cleanliness	1	2	1
8	Maturity of technology	2	5	1
8	Hover efficiency	8	8	7
3	Aerodynamic interaction	7	7	3
8	Vibration	2	2	2
7	Cruise efficiency	5	5	4
3	Maneuverability	9	9	10
9	Ease of payload packaging	8	8	7
10	Simplicity of structure	5	7	3
8	Simplicity of control system	10	10	4
	Total	621	687	362

Table 5. Other Helicopter Configurations

Weight	Selection Criteria	Rotor Wing	Tilt Rotor	Tilt Wing	Joined Wing
10	Compactness of folding	1	2	2	1
10	Reliability	1	3	3	1
8	Controllability	1	5	5	3
6	Aerodynamic cleanliness	6	2	4	10
8	Maturity of technology	2	7	6	1
8	Hover efficiency	1	3	5	2
3	Aerodynamic interaction	7	3	3	1
8	Vibration	8	6	6	10
7	Cruise efficiency	8	10	10	4
3	Maneuverability	1	4	4	10
9	Ease of payload packaging	10	10	10	8
10	Simplicity of structure	1	1	1	3
8	Simplicity of control system	1	1	1	3
	Total	332	421	441	344

From Table 2, it is clear that the conventional main rotor-tail rotor configuration is the best choice among the four configurations. Although compactness in folding is adversely affected by the large size of the rotor required, the maturity of technology and aerodynamic efficiency favor the conventional configuration.

Tip-jets, although attractive because of their simplicity of structure and ease of payload packaging, which is attributable to the absence of a power plant inside the fuselage, have the disadvantages of lower controllability and lack of compactness in folding. The lower controllability of tip-jets may be attributed to the lower lock number of the blade because of the high blade inertia resulting from blade-mounted nacelles[2].

5.1.2.2 Twin Rotor Configurations

Four twin rotor configurations were analyzed: side-by-side rotors, tandems (e.g., Boeing Chinook), coaxials (Kamov, Sikorsky) and ducted coaxial configurations (Sikorsky Cypher). Tandem helicopters have not been used for UAV designs. Coaxial configurations are the most widely used configurations for UAV design [8]. Sikorsky's Cypher and Cypher II [9], which have ducted coaxial configurations, are some of the most successful UAV designs.

The coaxial design is favored by most of the key design criteria and has received the highest number of points in Table 3. Side-by-side and tandem configurations also received comparable ratings. The difficulty of folding and the complexity of the structure are among the key disadvantages of these configurations. Ducted coaxial configurations, although well suited for UAVs, have significant compactness problems for a shell-launched mission. The shell length limits the rotor diameter to approximately 20 inches. Shrouds and ducts reduce the effective diameter of rotors, so these options cannot be folded efficiently to be packaged inside the 155-mm shell.

51.2.3 Quad Rotor and Other Rotor Configurations

Recently, the rotorcraft industry has been interested in designing rotorcraft with four or more lifting rotors. Varying the revolutions per minute of different rotors to change the direction of the thrust vector could control such configurations. Also, gyroscopes could be used to establish stability in forward flight. Some of the tested configurations are the Mesicopter [10], Gyronsaucer [11], and Roswell Flyer [12]. The latter two are radio-controlled helicopters and are reported to have very good controllability. The former (Mesicopter), a meso-scale flying machine that is no larger than a penny, is still in the developmental stage. In addition, a six-rotor version of the Mesicopter is proposed to improve its controllability. Table 4 indicates that a quad rotor design with free flying rotors has good potential to meet the design criteria. Free flying rotors are generally better than their shrouded counterparts in their simplicity of structure and aerodynamic cleanliness, as well as the amount of thrust generated per unit rotor diameter.

---

[2] streamlined enclosures (as for an engine) on an aircraft

5.1.2.4 Hybrid Helicopter Configurations

The candidates in the compound helicopter category are a rotor wing or stopped rotor [13], tilt-rotor (XV-15), tilt-wing and joined wing, and toroid[3] rotor configurations [14]. All these designs prove difficult to fold because of the large size of their wings. They are well suited for payload packaging and are very effective in high-speed forward flight conditions. However, since the mission plan does not require high-speed forward flight, these designs are not suitable options as configurations for SMARS.

5.1.3 Selection

A cursory look at the tables shows that the quad rotor and coaxial designs are the best candidates for the present design problem. The coaxial configuration has the advantages of compactness of folding and ease of deployment, while the quad rotor is superior from a controllability viewpoint. However, given the strength of the compactness requirement, the folding problems associated with the quad rotor preclude its use in this application. Therefore, the final configuration chosen for the SMARS vehicle is a coaxial rotorcraft.

5.2 Low Reynolds Number Airfoil

The requirements that drive the design of a low Reynolds number airfoil for SMARS are as follow:

- Rotor diameter is limited by stowage requirements;
- Blade Reynolds number must be maximized;
- Tip speed must be as high as possible but below the critical Mach number;
- High lift coefficient; and
- Low suction pressure peak.

Given these requirements, the best blade planform has a low aspect ratio, a parabolically swept 20% tip region, and positive blade taper. In addition, nonlinear twist should be incorporated to obtain a smooth lift coefficient distribution, and boundary layer trips should be used on both top and bottom surfaces to keep the flow attached. Finally, the airfoil should have a 6% camber and a 15% thickness and should spread the lift over the entire chord. The Alfred Gessow Rotorcraft Center (AGRC) 1506[1] was designed to fulfill the requirements and operate over the entire flight envelope of the SMARS vehicle (see Figure 7).

[3] a surface generated by a plane closed curve rotated about a line that lies in the same plane as the curve but does not intersect it

5.3 Coaxial Rotor Design

A detailed design study was performed to determine the coaxial rotor configuration and characteristics required to meet the specifications presented in the BAA. The rotor blade presented in the previous section was used, and a three-bladed rotor was assumed to ensure stability. The results of this study are presented in Table 6.

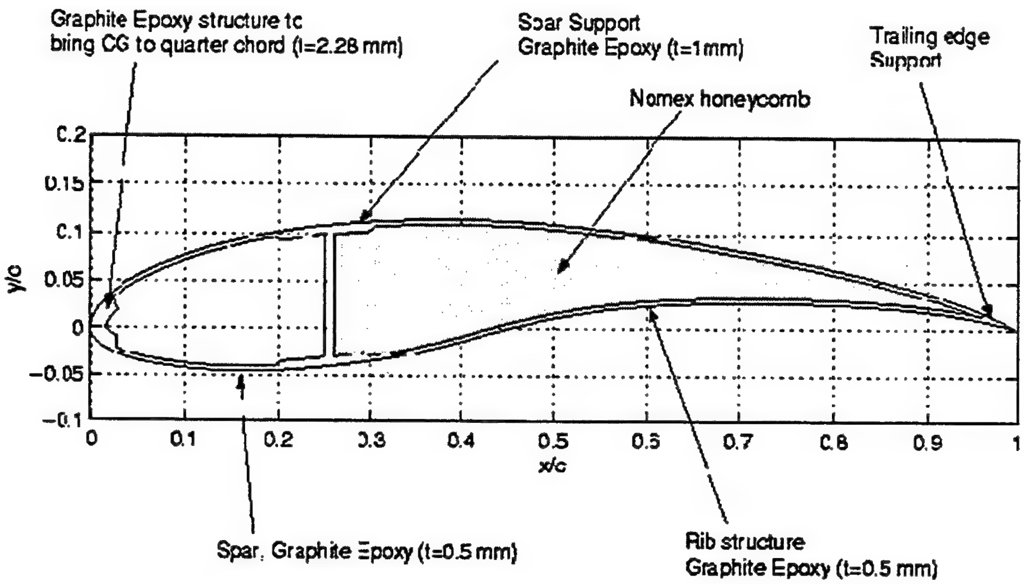

Figure 7. Airfoil AGRC 1506.

Table 6. Coaxial Rotor Characteristics

Parameter	Value
Number of blades	3
Radius	0.3015 m (1 ft)
Thrust coefficient	0.006 (each rotor)
Thrust-weighted solidity	0.136 (each rotor)
Disk loading	20.9 kg/m^2 (1.59 lb/ft^2) (each rotor)
Power loading	27.6 kg/kW (17.02 lb/hp)
Maximum Reynolds number	136,000
Tip Mach number	0.5
Effective aspect ratio	7.5
Hover power	1600 W
Forward flight power	1600 W

5.4 Propulsion System

To produce the required power specified in the previous section, many options are available, including electric motors, internal combustion engines, turbines, thermopiles, chemo-mechanical engines, remote powering methods, fuel cells, and compressed gas. All these options are able to produce the required power with a reasonable system weight, although some have higher power densities than others. However, in addition to power density, the propulsion system for SMARS must be readily available (low cost), highly reliable, must have a reasonably long shelf life and minimal complexity. Thus, it was felt that battery-driven electric motors were the best option.

A number of batteries were studied for SMARS and it was found that lithium-based batteries had the highest power density. The lithium batteries selected for the SMARS design study have a power density of 200 w/kg. However, one concern with lithium batteries is their poor discharge rate. MAVs require high discharge rates during flight operation. Therefore, a preliminary study of lithium battery discharge characteristics was performed. The goal of this test was simply to understand the discharge characteristics of lithium batteries, not to evaluate a specific battery for the vehicle. Power versus time was measured for a set of three lithium-ion batteries. Each battery was rated at 3.2 V with a capacity of 800 ma/hr. These batteries were chosen since they were readily available to the research team. The result of this experiment is provided in Figure 8. This figure shows that after an initial power drop-off, the battery power remains constant for a reasonable period of time. Thus, lithium batteries should be sufficient for SMARS.

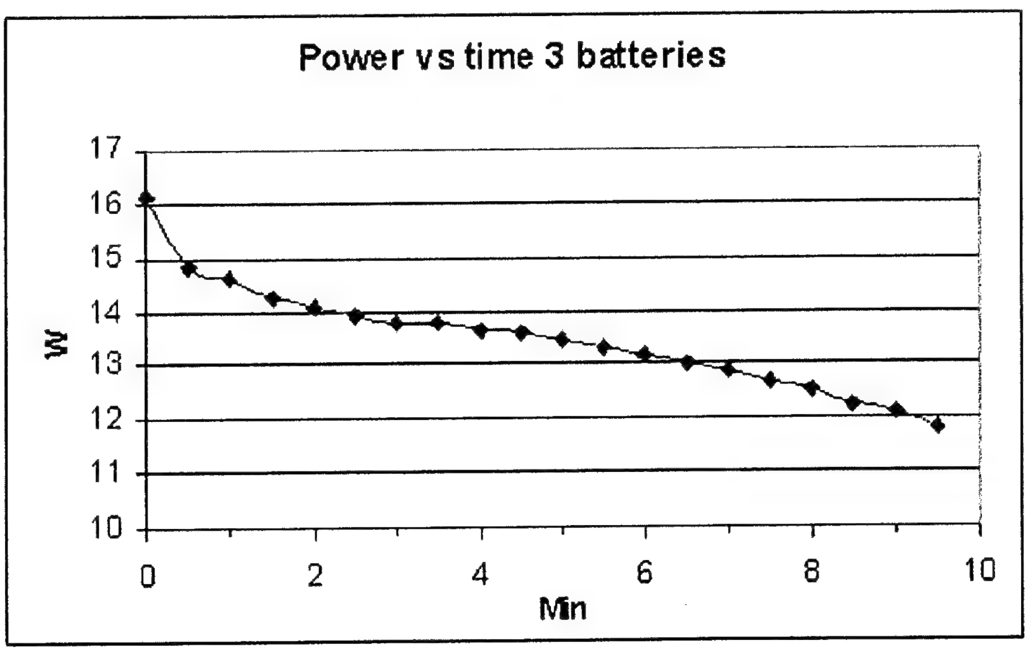

Figure 8. Lithium-Ion Battery Discharge Characteristics.

Both direct current (DC) and rotating field motors were considered for SMARS. DC motors have a number of advantages over rotating field motors, specifically,

- Current increases linearly with load,
- Higher expected efficiency,
- Higher starting torque, and
- Motor speed can be easily controlled.

However, DC motors have some common problems, including a limited lifetime, electrical interference and unreliable contacts. Most of these problems are associated with the motor brushes. Therefore, brushless DC motors were selected for SMARS since they combine the positive properties of DC motors with the robustness of rotating field motors.

5.5 Vehicular Parameters

Given the rotor parameters and the propulsion system selection, the vehicular parameters can be set. The parameters for SMARS are given in Table 7, and a preliminary drawing of the vehicle is presented in Figure 9.

Table 7. SMARS Vehicular Parameters

Parameter	Value
GTOW	6 kg
Battery weight (200 wh/kg)	4 kg
Empty weight	1 kg
Payload weight	1 kg
Hover power	1600 w
Forward flight power	1600 w
Mission duration	20 to 40 minutes

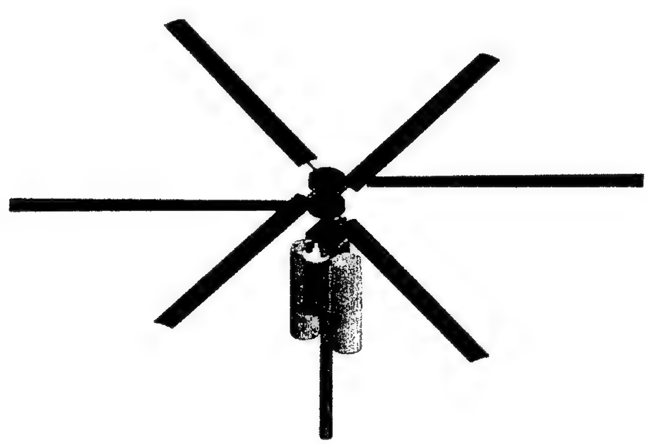

Figure 9. SMARS With No Lateral Control.

5.6 Packaging and Deployment

Packaging and deployment are two of the primary drivers in the development of the SMARS vehicle. As stated in the BAA, the vehicle must be packaged within an artillery shell. Thus, the stowed size of the vehicle must be no more than 147.8 mm (5.82 in.) in diameter and 406.4 mm (16 in.) in length. In order to accommodate this requirement, the SMARS rotor blades must be allowed to fold (see Figure 10).

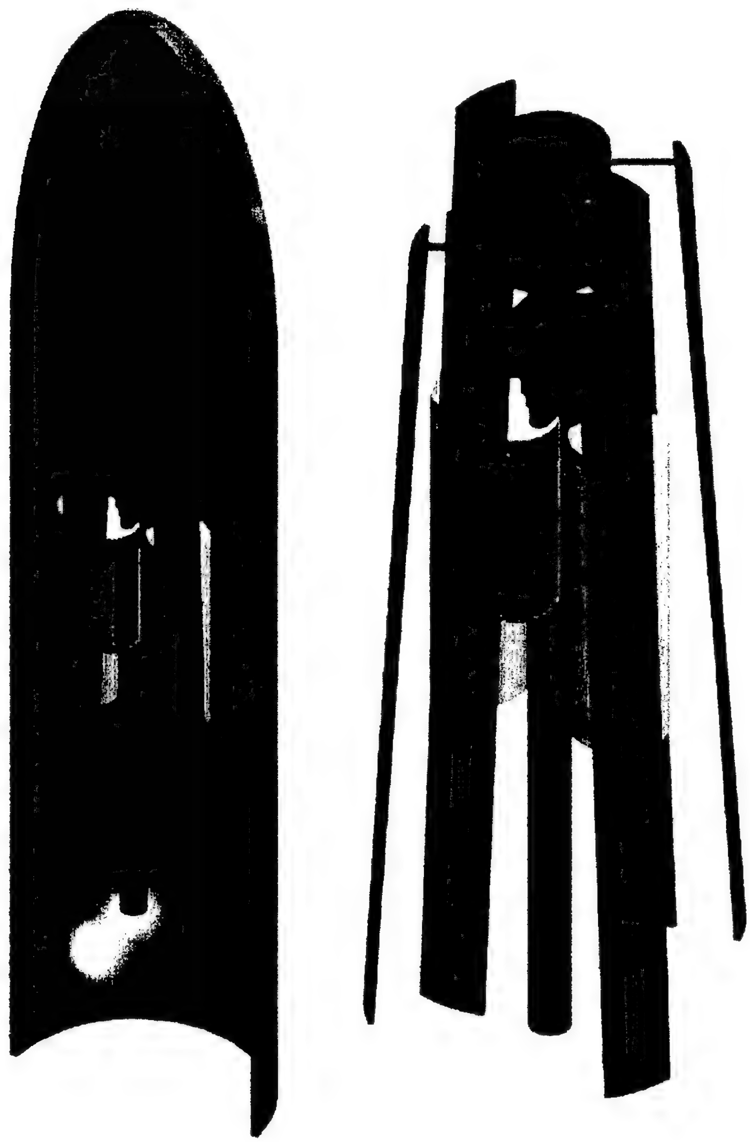

Figure 10. SMARS in Stowed Configuration.

The scheme for deployment of the smart submunition is displayed in Figure 11. Upon reaching an altitude of 3.5 km, the submunition canister is jettisoned from the artillery shell, and a parachute is deployed to slow and stabilize the descent of the submunition. While a parachute has been chosen in this initial study, a parafoil may be useful to guide the vehicle as it descends to the appropriate location. Once it reaches the observation location, the parachute is released and the submunition ejects the coaxial rotorcraft.

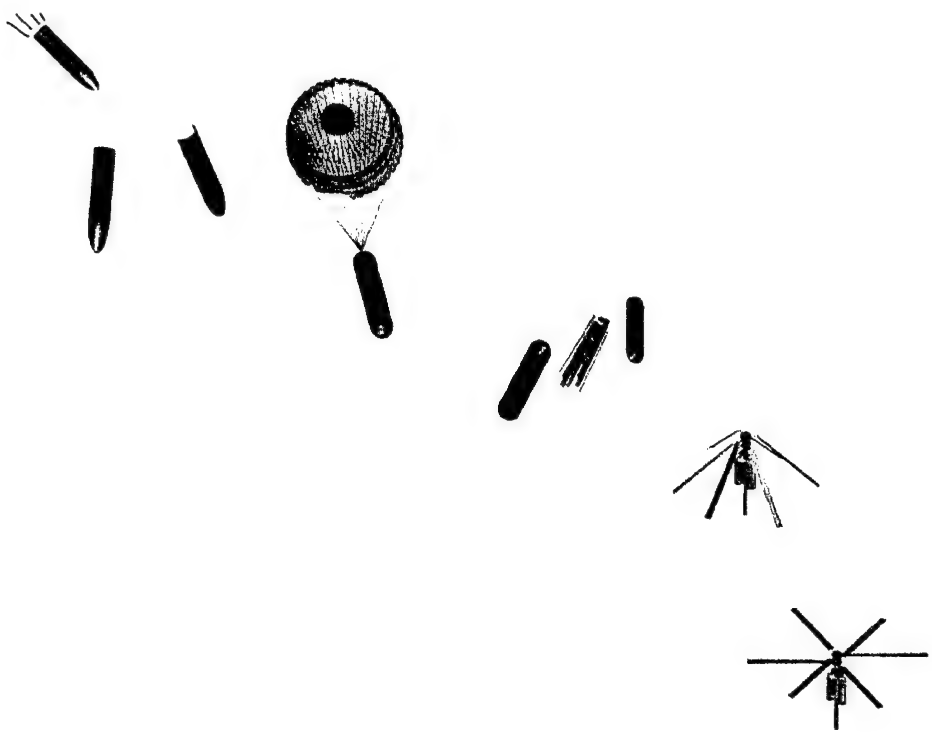

Figure 11. SMARS' Deployment Scheme.

5.7 Flight Control

A fully functional flight control is an absolute necessity for SMARS, given the mission requirements specified in the BAA. A typical rotorcraft control system (swashplate, pitch links, etc.) is quite complex; this is especially true for a coaxial rotor configuration. However, this complexity is prohibitive since it would significantly decrease the reliability and survivability of the vehicle. To simplify the mechanical design, the swashplate is eliminated and the rotors are completely rigid during flight. Thus, a non-traditional flight control system must be developed.

5.7.1 Yaw and Thrust Control

We can control yaw and thrust (altitude) by varying the revolutions per minute of the rotors. We can control yaw by varying the difference in revolutions per minute between the two rotors while we adjust thrust by varying the rotor revolutions per minute in tandem. This system requires each rotor to be driven

by a separate motor. The resulting transmission and motor configuration are presented in Figure 12.

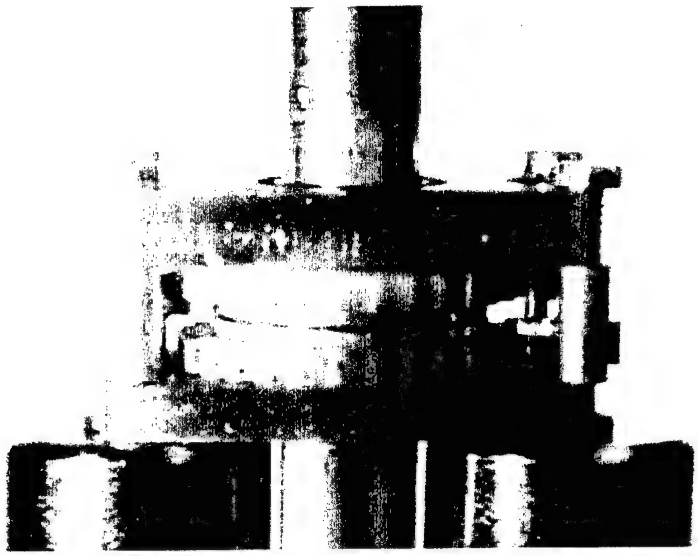

Figure 12. SMARS' Transmission Configuration.

5.7.2 Lateral Control

A number of lateral control methods were considered for the SMARS vehicle, including aerodynamic surfaces (flaps) for thrust vectoring, a gimballed drive train for thrust vectoring, and ducted fan and/or reaction jets to impose rolling and pitch moments. These three proposed systems were considered from the standpoints of mechanical complexity, control algorithm complexity, and power required. The control systems are shown in Figures 13, 14, and 15, respectively.

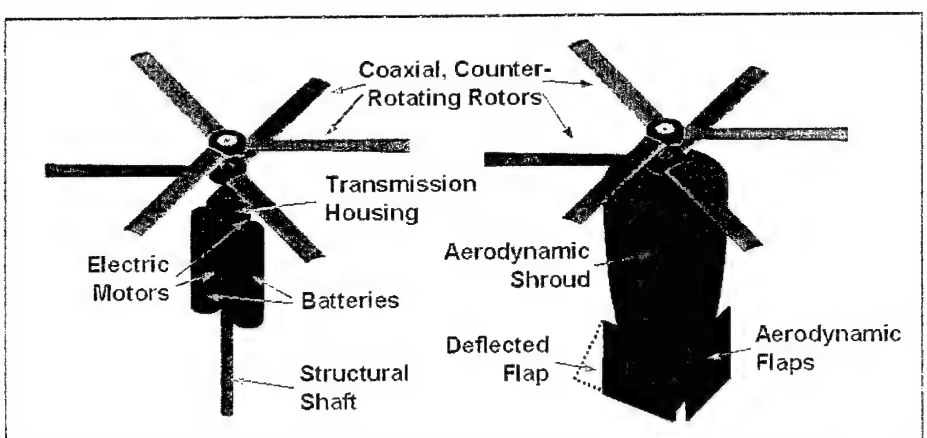

Figure 13. Aerodynamic Flaps.

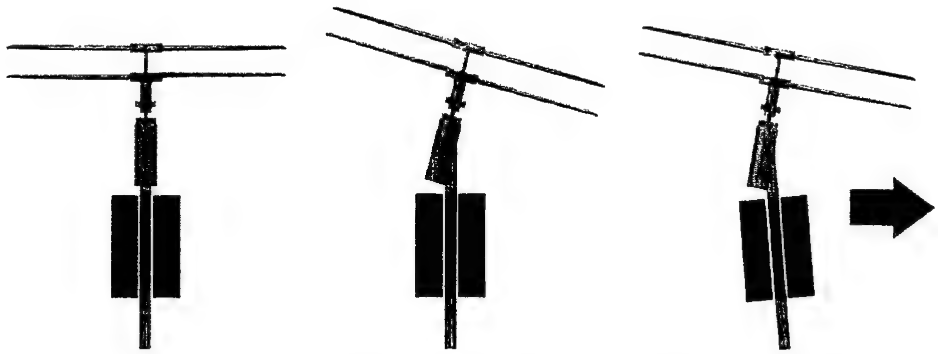

Figure 14. Gimballed Drive Train.

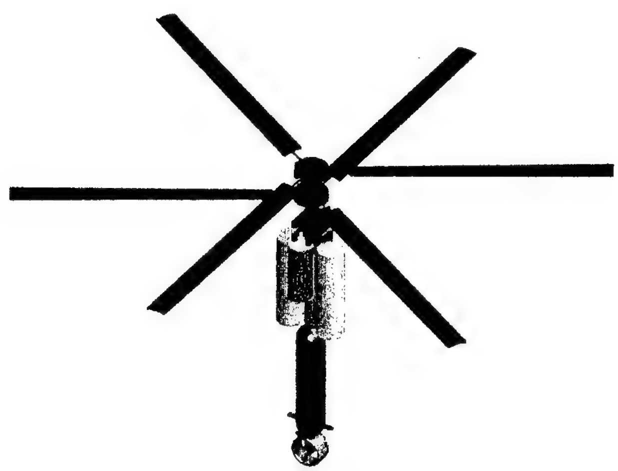

Figure 15. Ducted Propeller With Reaction Jets.

Of the three systems, the aerodynamic flap system would be the easiest to implement and seems to require only a small amount of power to operate. A more traditional control scheme would be to use fins that are mounted perpendicular against the fuselage, extended into the rotor downwash[4].

However, flap control was chosen instead of fin control for two reasons. First, the flap system fulfills the compact packaging requirements since (except during maneuvers) the flaps remain flush to the fuselage. Second, when not maneuvering, the flaps remain out of the rotor wash[5], thereby reducing drag and increasing hover efficiency. Extension of the flaps creates a torque, which is used to control the attitude of the vehicle in pitch and roll. Development of stability and control algorithms via this control method was determined to be a manageable problem.

[4] an air stream directed downward (as by an airfoil)
[5] the wind and vortices caused by the rotor blade moving through the air

The gimballed drive train system, though slightly more complex than the aerodynamic flap system, ultimately yields the cleanest final vehicle configuration and potentially requires the least amount of power to operate. Once again, the development of stability and control algorithms via this control method was determined to be a manageable problem.

The preliminary study indicated that the ducted propeller with reaction jet system would require significantly more power than the previous two systems, so it was not considered further in this report. A study of the effectiveness of the remaining two control systems is presented in Section 6.3.

6. Small-Scale Prototype Study (MICOR)

As part of a parallel project, a small-scale radio-controlled coaxial rotorcraft (MICOR) was manufactured and partially flight tested. This vehicle shares many design characteristics with the SMARS vehicle. The following section presents an overview of MICOR and demonstrates that it can be effectively enlarged to meet the size requirements for the SMARS vehicle.

6.1 Vehicle

The prototype MICOR vehicle, displayed in Figure 16, has a coaxial rotor with an axisymmetric fuselage. To simplify the mechanical design, the swashplate is eliminated and the rotors are completely rigid during flight. However, for packaging reasons, the blades must be capable of being stowed against the fuselage when they are not in use. While this feature has not been incorporated in this initial design, a folding blade mechanism has been designed and will be incorporated in future vehicles.

6.1.1 Rotor Blades

The prototype rotor blades were designed primarily for ease of manufacture. Therefore, a thin airfoil with 8% constant radius camber was chosen. Each blade has a chord of 1 cm and a length of 7 cm. The blades consist of three layers of graphite-epoxy weave with a fiber orientation of +45°, 0°, +45°. A simple mold composed of a top concave surface, a bottom convex surface, and an edge dam was made from aluminum (see Figure 17).

The composite was placed in the mold, clamped and cured. The resulting blades are very consistent and require only minimal post-cure processing. Finally, a small aluminum pin was bonded to the root of the blade. The root pin has a flat surface along a portion of its length to aid in bonding, and the end opposite the flat surface is flared to transfer axial loads from the blades to the hub.

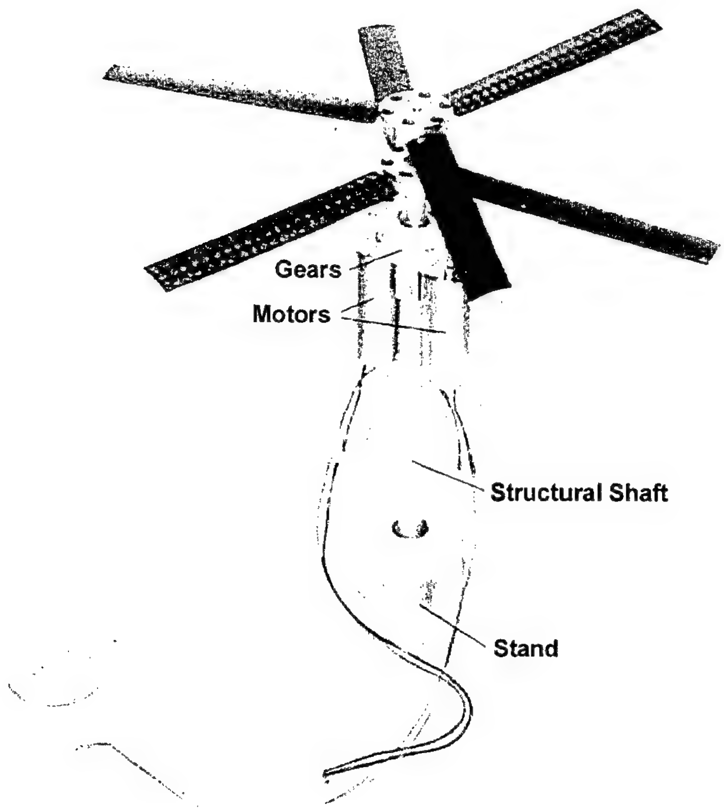

Figure 16. MICOR.

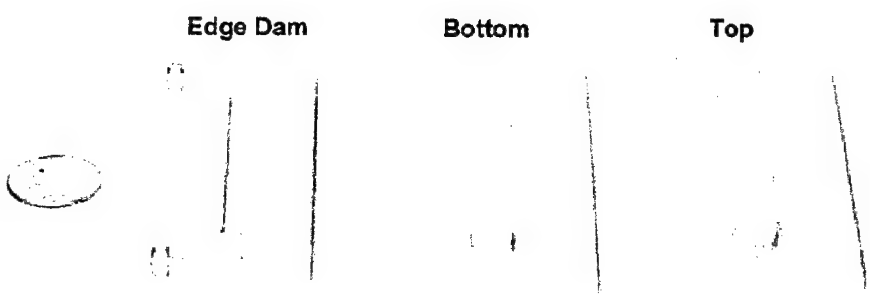

Figure 17. Blade Mold Parts.

6.1.2 Rotor Hub

The rotor hub consists of two parts, top and bottom, that clamped onto the root pin, constraining its rotation and thus fixing the angle of attack of the blades. A space was left in the hub for the flared end of the root pin. This design allows the

blade angle of attack to be changed between flights in order to determine the best angle of attack for each rotor. In addition, it is easy to change rotor blades and test different blade designs. Once the best blade geometry has been determined, the blade-hub assembly will be manufactured as a single part, and the blade-folding mechanism will be incorporated.

6.1.3 Transmission and Fuselage

The vehicle configuration requires each rotor to be driven by a separate motor. To accomplish this, a transmission was designed and manufactured in house. The final transmission configuration is shown in Figure 18. The transmission design consists of an eight-tooth pinion and a 30-tooth gear, resulting in a reduction ratio of 3.75:1. In addition to providing the desired reduction ratio, this configuration provides enough space between the motors for the structural shaft. The transmission housing was designed to support the gears, rotor shafts, and motors and transmit the rotor loads from the rotor system to the fuselage. The fuselage consists of a structural shaft mounted on the bottom of the transmission housing. This shaft provides additional support to the motors as well as support to the batteries, lateral control system, control electronics and payload.

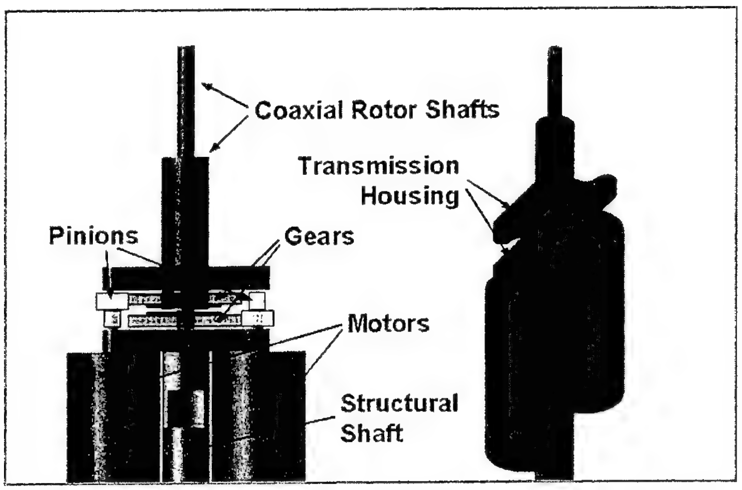

Figure 18. Final SMARS' Transmission Configuration.

6.2 Tethered Flight Test

To date, a lateral control system has not been implemented on this version of MICOR. Therefore, this vehicle has been used to demonstrate the feasibility of the concept and validate the effectiveness of the thrust and yaw control systems. For all these tests, the vehicle was flown along a vertical cable in order to constrain its lateral motion. This was necessary because there was no lateral control system. Two flight tests were performed, the first using tethered power and the second using on-board power.

The tethered power flight test (see Figure 19) used power supplied to the electronics via a cable from a DC power supply. During this test, altitude and yaw control, as well as yaw stability via a piezoelectric gyroscope, were demonstrated. This test ended before the batteries were depleted because the lateral constraint cable failed. However, the remaining battery power was measured, and it was determined that the vehicle could have flown for approximately 10 minutes.

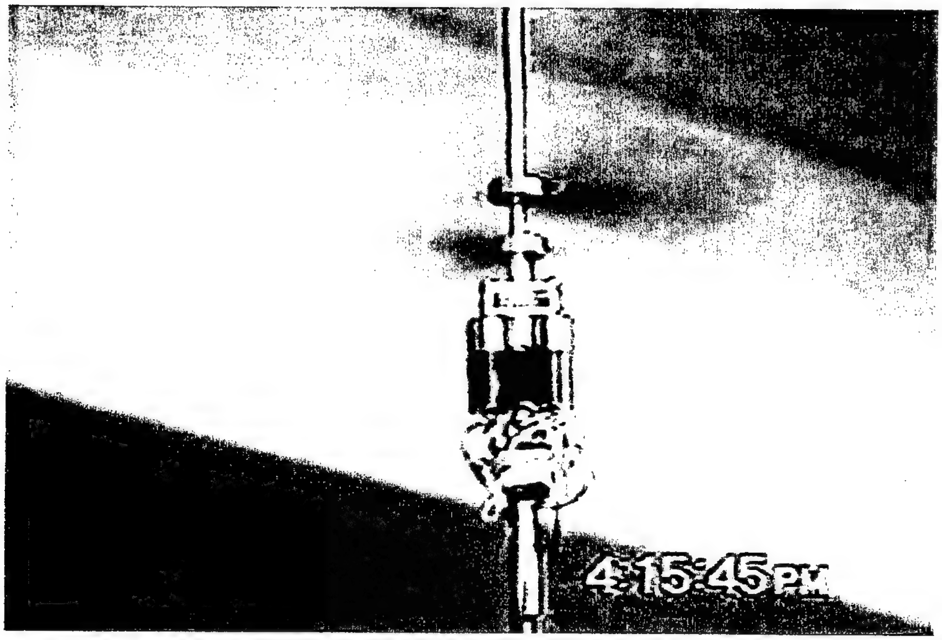

Figure 19. Tethered Flight Test.

6.3 Lateral Control and Scaling

Two of the lateral control systems mentioned in Section 5.7, flaps mounted flush to the fuselage and a gimballed drive train rotor (hinged mass), have been studied for MICOR. First, the pitch and/or roll moments that each configuration can generate are estimated for a general vehicle. Next, values for disturbance moments generated by gusts are estimated. Finally, the effect of scaling on the relative effectiveness of each vehicle is investigated.

6.3.1 Available Control Moments

Two potential configurations for lateral (pitch and roll) control of a small coaxial rotorcraft are a hinged mass and aerodynamic flaps. In the hinged mass configuration, the plane of the rotor system is tilted with the use of servos, thus reorienting the thrust vector and causing body moments. In the aerodynamic flap configuration, deflecting flaps in the rotor downwash generates moments. The following analysis predicts the magnitude of the moments that each system can generate and then discusses whether we expect these moments to translate to

sufficient bandwidth for a coaxial rotorcraft in a noisy environment. The entire analysis is performed for the simplified case of the vehicle in hover.

The moment generated by a deflection of the thrust vector by Θ_T degrees is simply

$$T_T = d_T T \sin \Theta_T.$$

Typical values for MICOR are easily found. Thrust equals the weight of the system (approximately 1 newton). To maximize available moments in this configuration, the heaviest components would be placed near the bottom of the vehicle to maximize d_T. Assume that a d_T of 10 cm is achievable. Finally, a typical value must be chosen for Θ_T. Considering that for practical purposes we do not want the vertical component of thrust to change by more than a few percent, a generous upper boundary for Θ_T is 15 degrees. Therefore, substituting in these values, the maximum expected moment is

$$M_T = 0.026 \text{ newton-meter}$$

For the aerodynamic flap configuration, the moment generated by a fin force F_f is simply $d_f F_f$. If we assume that the flaps have a constant lift curve slope of $C_{l\alpha}$, then the moment for a flap deflection of α becomes $1/2 d_f\, C_{l\alpha}\, \alpha \rho V^2 A_f$, in which V is the local wind velocity and A_f is the surface area of the flap. If we further assume that the flaps operate in the fully contracted rotor wash, then from simple momentum theory, V becomes $(2T/\rho A_r)^{1/2}$, in which ρ is the air density and A_r is the surface area of the rotor disk. Therefore, the total moment attributable to the flaps can be written

$$M_f = T A_f d_f C_{l\alpha} \alpha / A_r$$

For this configuration, we place the center of gravity of the vehicle as close to the rotors as possible and place the flaps far from the rotors. With this strategy, a d_f of 10 cm should be achievable. Given a typical rotor diameter of 15 cm and air density at sea level of 1.225 $\text{kg}/_m{}^2$, flap surface expected maximum moment attributable to flaps at hover is

$$M_f = 0.035 \text{ newton-meter}$$

The typical fin surface area of 50 cm^2 is generated by the assumption of two fins of surface area 25 cm^2 on either side of the fuselage and deflecting in the same direction. If the flaps are mounted flat against the fuselage so that only one could be deflected, the available moments are cut in half.

Considering the extremely simplified nature of moment approximations, the one-third greater estimated moment of the flap configuration is somewhat negligible. The interesting result is that each configuration produces moments of approximately the same magnitude, at around a few hundredths of a newton-

meter. A more detailed analysis would consider numerous additional factors, including better approximations of the rotor wash velocity and available flap forces. In practice, it is easier to move the center of gravity closer to the rotor than farther away since the transmission and motors must necessarily be situated near the rotor. This tends to favor the aerodynamic flap configuration.

Next, an estimation of the moment required to sufficiently control the vehicle must be performed. The desired bandwidth should be relatively large in order to provide a measure of robustness to disturbances in the system. From knowledge of our vehicle, we can estimate values for I and $(w_c-\omega)$ and specify a desired bandwidth B, thus yielding the required value for the commanded moment $M_c = 0.0126$.

This analysis indicates that expected control moments available from MICOR are safely larger than control moments required for MICOR, in either a hinged mass or aerodynamic flap configuration.

Thus, the effectiveness of the control moments (the ratio of control to disturbance moments) is more than sufficient to maintain control of the vehicle. This is true even given the somewhat large desired bandwidth requirement. In fact, double the desired bandwidth would still yield acceptable required moment commands.

6.3.2 Scaling

In order to compare M_T to M_f for similarly scaled vehicles, we must make a few assumptions. First, assume that when the vehicle is scaled, all dimensions are scaled equally. Therefore, thrust T, which equals the weight of the vehicle in hover, scales with the cube of some reference dimension on the vehicle. For this analysis, let the moment arms df and dT be equal and let them be the reference distance d. Thus, thrust can be written T = CTd3. Rewriting the expressions for MT and Mf with this expression for T, we have

$$M_T = C_T d^4 \sin \Theta_T.$$
$$M_f = (C_T d^4 A_f C_{1\alpha} \alpha)/A_r.$$

The ratio of moments (with a hinged mass system) to moments from an aerodynamic fin system is therefore

$$M_T / M_f = (A_r / A_f)(\sin \Theta_T . / C_{a\alpha} \alpha)$$

It is clear that the ratio is independent of the scale d.

Now we generate estimates for disturbance moments on the vehicle. Assume that all the moments result from drag on the vehicle in the presence of a gust of velocity V_g. Therefore, the disturbance moment M_d can be written

$$M_d = 1/2 C_d \rho V_c^2 A_d d_d$$

in which C_d is the coefficient of drag, ρ is the air density, A_d is the reference area, and d_d is the moment arm from the net drag force vector to the vehicle center of gravity. In order to create a scaling law for disturbance moments, the expression for M_d should be written in terms of the reference distance d. Since the reference area A_d is proportional to d^2, and d_d is directly proportional to d, we can let $C_d A_d d_d = C_m d^3$ in which C_m is the coefficient of moment for the vehicle with reference scale d. Substituting into the expression for M_d, we have

$$M_d = (1/2) C_m V_d^2 d^3$$

Note that the disturbance velocity V_d does not scale, since it is a function of the environment. The coefficient of moment can be assumed to be constant in this simple analysis, but in reality, it will not be exactly the same for each vehicle, since the aerodynamic flap setup will experience larger moments because of the large aerodynamic surfaces. The significant result of this analysis is that the control moments scale with d^4, while the disturbance moments scale with d^3. Thus, the effectiveness of the control moments provided by both systems scales linearly with increased vehicle size.

Finally, with this scaling result and given that MICOR can generate sufficient control moments and that the SMARS vehicle is larger than MICOR, SMARS should have no problem generating moments sufficient for lateral control.

6.3.3 Result

The results of this analysis can be summarized in the following three points:

1. The control moments generated by both systems are of the same magnitude.

2. The control moments generated by a system implemented at the scale of MICOR are sufficient to maintain control of the vehicle.

3. The control moments scale linearly with vehicle size. Thus, the SMARS vehicle, which is larger than MICOR, should have no problem generating moments sufficient for lateral control.

7. Deployment Feasibility Study

A simple test was devised to demonstrate the feasibility of deploying a rotorcraft from a munition. The test consisted of developing a simple, unpowered, rotary

wing vehicle with folding blades that could be launched by and deployed from a high-powered model rocket.

7.1 Vehicular Parameters

The vehicle developed for this test is shown in Figure 20. This vehicle is approximately the size of the SMARS vehicle. While stowed, the blades of the rotorcraft fold (see Figure 21). When deployed, the blades unfold and the vehicle auto-rotates to the ground.

Figure 20. SMARS Test Vehicle.

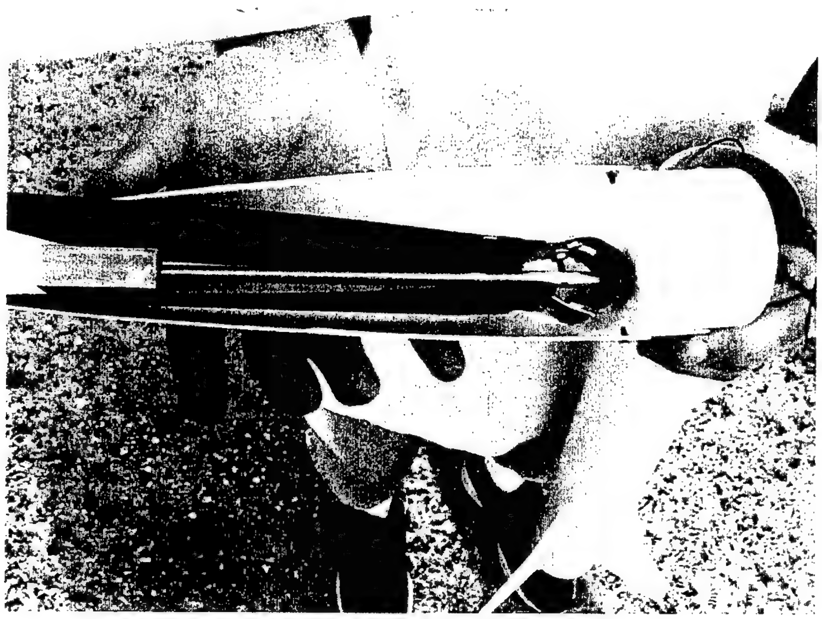

Figure 21. SMARS Test Vehicle in the Stowed Configuration.

7.2 Launch System

A high-powered Aerotech model rocket (see Figure 22) was used for this test. The nose cone was modified so that the rotorcraft could be stowed inside (see Figure 23). Upon ejection, the nose cone opened to deploy the rotorcraft. The rocket returned to the ground with a parachute.

Figure 22. Launch Rocket.

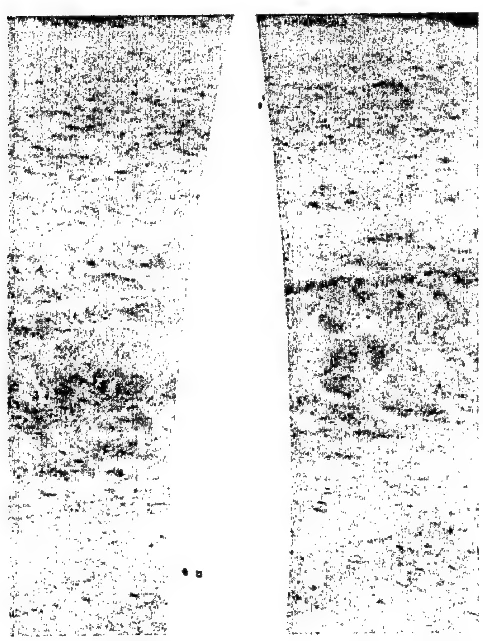

Figure 23. Test Vehicle Stowed in the Rocket Nose Cone.

The motor used to power the rocket was an F-size Aerotech composite solid rocket motor. This motor propelled the rocket to approximately 1000 ft and subjected it to 10 g's.

7.3 Flight Test

Four successful flight tests were performed. Each time, the rotorcraft was deployed and both the rocket and the rotorcraft were retrieved with only minor damage.

8. Conclusion

Design and analysis of the SMARS vehicle, a rotorcraft designed for deployment from a conventional munition, have been detailed in this report. SMARS was designed in response to requirements defined in an initial meeting with Mr. Michael Hollis of the U.S. Army Research Laboratory, Aberdeen Proving Ground, Maryland, on April 18, 2000.

The primary goal of this design study was to develop a rotorcraft that could be housed inside a conventional munition and carry a payload of 1.36 kg over a period of 20 minutes. The vehicle must be capable of scanning an area equivalent to 5 km^2.

The final design concept consists of a coaxial rotorcraft with a 0.6096-m (2-ft) rotor diameter weighing 6 kg. Rotors are rigid in flight; the swashplate was eliminated to reduce complexity. However, the blades are able to fold at the root in order to meet packaging requirements. The propulsion system consists of two brushless electric motors powered by lithium batteries weighing a total of 4 kg. Each motor drives a single rotor via a transmission designed in house. Yaw and altitude control is accomplished by the changing of the revolutions per minute of the rotors. Lateral control is accomplished via aerodynamic flaps or by a gimballed drive train.

A small-scale prototype called MICOR was developed and flight tested to show the feasibility of the concept and to validate the yaw and altitude control systems. Scaling laws were developed to ensure that the characteristics of MICOR could be applied to SMARS. In addition, a deployment feasibility study was performed. A simple small-scale rotorcraft was manufactured. This vehicle was launched and deployed by a high-powered model rocket to demonstrate the feasibility of the SMARS concept.

Much work remains to be done in the development of SMARS. However, the research team feels that this report presents a feasible concept for a smart submunition that could become operational in the near future.

INTENTIONALLY LEFT BLANK

References

1. "The Martian Autonomous Rotary-Wing Vehicle (MARV)," Design Report, Alfred Gessow Rotorcraft Center, University of Maryland, College Park, MD, June 1, 2000.

2. Smith, J.O., K.M. Black, F.A. Kamangar, and J. Fitzer, "The University of Texas at Arlington, Autonomous Aerial Vehicle – An Overview," Journal of Applied Intelligence, Vol. 2, 1992.

3. Web Site, http://209.207.236.112/irp/program/collect/vtuav.html.

4. Stepniewski, W.Z., and T. Tarczynski, "Open Airscrew VTOL Concepts," NASA Contractor Report NASACR-177603, International Technical Associates Ltd, Drexel Hill, PA. National Aeronautics and Space Administration, Washington, DC, September 1992.

5. Web Site, http://www.planetinternet.be/pixel/.

6. Web Site, http://www.dragonflypictures.com/.

7. Woodley, B., H. Jones, E. Frew, E. LeMaster, and S. Rock, "A Contestant in the 1997 International Aerial Robotics Competition," ALUVSI 1997 Proceedings, July 1997. Aerospace Robotics Laboratory, Stanford University, at web site http://sun-valley.stanford.edu/users/heli/.

8. Web Site, http://www.naval-technology.com/projects/seamos/seamosl.html.

9. Web Site, http://www.army-technology.com/projects/cypher/cypherl.html.

10. Kroo, I., and F. Prinz, "Mesicopter Project: Research and Development Work in the Area of Ultra-Low Reynolds Number Aerodynamics," Progress Report, web site, http://aero.stanford.edu.mesicopter/,1999.

11. Web Site, http://www.keyence.co.jp/international/hobby/saucer.html.

12. Web Site, http://www.afot.com/.

13. Web Site, http://larcpubs.larc.nasa.gov/randt/1993/RandT/SectionD/D7.html.

14. Stancil, C.M., "Electric Toroid Rotor Technology Development," at web site, http://www.naic.usra.edu/files/studes/abstract/56Stancil.html.

INTENTIONALLY LEFT BLANK

NO. OF COPIES | ORGANIZATION

1 ADMINISTRATOR
DEFENSE TECHNICAL INFO CTR
ATTN DTIC OCA
8725 JOHN J KINGMAN RD STE 0944
FT BELVOIR VA 22060-6218

1 DIRECTOR
US ARMY RSCH LABORATORY
ATTN AMSRL CI AI R REC MGMT
2800 POWDER MILL RD
ADELPHI MD 20783-1197

1 DIRECTOR
US ARMY RSCH LABORATORY
ATTN AMSRL CI LL TECH LIB
2800 POWDER MILL RD
ADELPHI MD 20783-1197

1 DIRECTOR
US ARMY RSCH LABORATORY
ATTN AMSRL D D SMITH
2800 POWDER MILL RD
ADELPHI MD 20783-1197

1 DIRECTOR
US ARMY RSCH LABORATORY
ATTN AMSRL RO EN
T DOLIGALSKI
DURHAM NC 27709-2211

ABERDEEN PROVING GROUND

2 DIRECTOR
US ARMY RSCH LABORATORY
ATTN AMSRL CI LP (TECH LIB)
BLDG 305 APG AA

5 DIRECTOR
US ARMY RSCH LABORATORY
ATTN AMSRL WM BA M HOLLIS
BLDG 4600

8 DIRECTOR
US ARMY RSCH LABORATORY
ATTN AMSRL WM BC P PLOSTINS
M BUNDY D LYON
B GUIDOS T ERLINE
J SAHU D WEBB
P WEINACHT
BLDG 390

NO. OF COPIES | ORGANIZATION

ABSTRACT ONLY

1 DIRECTOR
US ARMY RSCH LABORATORY
ATTN AMSRL CI AP TECH PUB BR
2800 POWDER MILL RD
ADELPHI MD 20783-1197

INTENTIONALLY LEFT BLANK

REPORT DOCUMENTATION PAGE

Form Approved OMB No. 0704-0188

1. AGENCY USE ONLY *(Leave blank)*	2. REPORT DATE	3. REPORT TYPE AND DATES COVERED
	June 2001	Final

4. TITLE AND SUBTITLE

Feasibility Study of a Smart Submunition: Deployment From a Conventional Weapon

5. FUNDING NUMBERS

AMS: 622716
PR: AH70

Contract No. DAAD19-00-1-0127

6. AUTHOR(S)

Wereley, N.M.; Pines, D.J. (University of Maryland)

7. PERFORMING ORGANIZATION NAME(S) AND ADDRESS(ES)

Smart Structures Laboratory
Alfred Gessow Rotorcraft Center
Department of Aerospace Engineering
University of Maryland
College Park, MD 20742

8. PERFORMING ORGANIZATION REPORT NUMBER

9. SPONSORING/MONITORING AGENCY NAME(S) AND ADDRESS(ES)

U.S. Army Research Laboratory
Weapons & Materials Research Directorate
Aberdeen Proving Ground, MD 21005-5066

10. SPONSORING/MONITORING AGENCY REPORT NUMBER

ARL-CR-0475

11. SUPPLEMENTARY NOTES

The contracting officer's technical representative (COTR) is Michael Hollis, U.S. Army Research Laboratory, ATTN: AMSRL-WM-BA, Aberdeen Proving Ground, MD 21005-5066 (telephone 410-306-0732).

12a. DISTRIBUTION/AVAILABILITY STATEMENT

Approved for public release; distribution is unlimited.

12b. DISTRIBUTION CODE

13. ABSTRACT *(Maximum 200 words)*

This report details the smart autonomous rotorcraft submunition (SMARS) designed for deployment from a conventional munition. SMARS was developed in response to requirements defined in an initial meeting with Mr. Michael Hollis of the U.S. Army Research Laboratory, Aberdeen Proving Ground, Maryland, April 18, 2000.

The primary goal of this initial design was to develop a rotorcraft that could be housed inside a conventional munition and carry a payload of 1.36 kg for a period of 20 minutes. The vehicle must be capable of scanning an area equivalent to 5 square kilometers. The proposed design in this report satisfies these requirements.

The final design concept consists of a coaxial rotorcraft with a 0.6096-m (2-foot) rotor diameter weighing 6 kg. The rotors are rigid in flight; the swashplate was eliminated to reduce complexity. However, the blades are able to fold at the root in order to meet packaging requirements.

A small-scale prototype called "miniature coaxial rotorcraft" (MICOR) was developed and flight tested to show the feasibility of the concept and validate the yaw and altitude control systems. Scaling laws were developed to ensure that the characteristics of MICOR could be applied to SMARS. In addition, a deployment feasibility study was performed. A simple small-scale wind milling rotorcraft was manufactured, which was launched and deployed by a high-powered model rocket to demonstrate the feasibility of the SMARS concept.

14. SUBJECT TERMS

guided flight SMARS
rotor configurations

15. NUMBER OF PAGES

40

16. PRICE CODE

17. SECURITY CLASSIFICATION OF REPORT	18. SECURITY CLASSIFICATION OF THIS PAGE	19. SECURITY CLASSIFICATION OF ABSTRACT	20. LIMITATION OF ABSTRACT
Unclassified	Unclassified	Unclassified	

NSN 7540-01-280-5500

Standard Form 298 (Rev. 2-89)
Prescribed by ANSI Std. Z39-18
298-102